

Visualizing Diffusion Tensor Dissimilarity using an ICA Based Perceptual Colour Metric

Mark S. Drew and Ghassan Hamarneh; School of Computing Science, Simon Fraser University, Vancouver, British Columbia, Canada V5A 1S6 {mark,hamarneh}@cs.sfu.ca

Abstract

Diffusion-tensor data from medical MR imaging consists of a 3×3 symmetric positive semi-definite matrix at each voxel. The issue of how to understand, and how to meaningfully display this type of data has been gaining interest since its development as a noninvasive investigative tool [1]. Several schemes have been developed, usually aimed at the display of the spatial geometric structure of each voxel characterized by its eigenvectors. However these efforts have used colour merely as a visualization device, without regard to an underlying metric structure between voxels. At the same time, some work has been developed on analyzing whole-brain structure using independent component analysis, making use of similarity between tensors to identify separated overall structures, e.g. for de-noising of spatial features. In this paper we consider using colour to understand these separated structures, mapping a true metric giving a similarity measure between tensors into a perceptually uniform colour space, so that colour difference corresponds to true difference. We show that such a colour map can better discriminate regions of distinct diffusion properties in the brain than previous methods.

1. Introduction

Diffusion tensor imaging is a recent modality utilizing magnetic resonance imaging to establish strength and direction of water-molecule diffusion paths in vivo [2]. A pair of sharp magnetic field gradient pulses can be used to establish the displacement of nuclei during the ‘diffusion time’ between the two pulses. The result is an array giving diffusion rates in the xx , xy , xz , ... zz directions in a patient-centered coordinate system. The resulting 3×3 array is called a Diffusion “Tensor” (DT) – simply an array, in fact, since no coordinate transformations are performed (cf. [3]). For physical reasons, these arrays are both symmetric and positive semi-definite.

Analysis of such data has included establishing reasonable metrics for gauging distance between tensors, and also on visualizing the tensor data. Several metrics have been developed [4, 5, 6] and, consequently, it is possible to perform segmentation, smoothing, and interpolation of such DT volume data based on these distances (see e.g. [7]).

Colouring schemes have been centered on visualizing the 3D structure of the array data: the fundamental analysis on such data is a principal component analysis of each separate voxel 3×3 array (using Singular Value Decomposition — SVD), identifying the first eigenvector with the main direction of diffusion at that voxel [8]. As well, the relative magnitudes of the set of three eigenvalues λ_i , $i = 1..3$ have been used to identify voxels as having a line-like ($\lambda_1 \gg \lambda_2 \simeq \lambda_3$), plane-like ($\lambda_1 \simeq \lambda_2 \gg \lambda_3$), or isotropic structure ($\lambda_1 \simeq \lambda_2 \simeq \lambda_3$) [9]. A key scalar feature developed from eigenvalue data is the Fractional Anisotropy (FA), capturing the degree of diffusion that is anisotropic as opposed to spherical [10, 11]. The trace of the diffusion tensor along with the FA have been useful for tractography [12], the segmentation and display of

diffusion-pathway organization, particularly in the brain.

Voxel colouring has centered around portraying the direction and strength of the principal eigenvector at each location [13]. A simple approach to this problem is to colour the three components of the first eigenvector according to a pre-determined colour map [13], or by multiplying the tensor by a fixed pre-specified probe vector and associating the 3-vector result with {R,G,B} [14]. To show the dimensionality and direction of the SVD decomposition, another approach has been to combine colour with an ellipsoid representation of the tensor [9]. Colour has also been weighted by the FA measure to show directionality and strength [15].

In these efforts, little attention has been paid to forming colours that actually correspond to a difference metric within the structure being imaged. Instead, colour is assigned in a straightforward way so as to visualize aspects of the DT data. An attempt [13] made to assign colour according to the CIELUV metric [16] was deemed “unsatisfactory”; and this is not surprising, since again the idea of mapping the principal eigenvector at each pixel into {R,G,B} was used, followed by an unspecified mapping to L^* , u^* , v^* , presumably by way of a mapping of monitor RGB colour to tristimulus values XYZ as in multimedia applications (see, e.g., [17]).

Another direction in investigating DT volume datasets has been to look at the whole dataset, rather than each voxel separately. In [18] an Independent Component Analysis (ICA) [19] was carried out on whole-brain data, as a preliminary analysis before traditional examination of the trace of the tensor and its FA. The idea was to find components related to noise, and remove them before reconstituting the tensor data from its decomposition. At the same time, it was determined that the primary ICA component identified the brain’s Cerebro-Spinal Fluid, and was less noisy than the trace-of-tensor map that had been used previously. Other ICA components mapped major groups of White Matter fibers. ICA has also been applied to Single Photon Emission Computerized Tomography brain data, identifying regions differing between healthy patients and those with Parkinson’s disease [20]; and applied to Functional MR data to identify regions of activation, with no prior knowledge of expected responses required [21]. Since ICA is a form of “blind source separation”, it has also been used in DT analysis to distinguish multiple White Matter fiber tracts that cross at voxel locations [22], automatically separating out the contributing components.

In this paper, we develop a method for mapping the full tensor data into three colour values, such that colour has meaning in terms of a difference metric that makes sense on diffusion tensor data. Symmetric 3×3 voxel data effectively has 6 unique elements. Since we are interested in mapping to colour, we must first find a reasonable mechanism for descending from 6D to 3D. Here, we go by way of an ICA analysis on whole-brain data. Since we have a tensor metric, we can map into a colour metric such that uniform perceptual colour differences map uniform tensor-

metric differences.

In §2 we briefly recapitulate ICA, as applied here to DT data, and outline an appropriate DT metric. With the help of ICA components, we map this metric into a perceptual colour metric in §3. Section 4 shows the efficacy of this colour-based understanding in an application, by showing that ICA-driven colour enhances the capability of segmentation of the corpus callosum. We draw conclusions in §5.

2. Log-Euclidean Metric and ICA

Diffusion Tensor Metric

As stated above, DT data consists of 3×3 symmetric matrix data at each voxel. Since diffusion is being measured, not all areas of the brain will show a DT signal of non-vanishing magnitude. So in visualizing this data it often helps to display DT MR imagery alongside conventional T1- or T2-weighted MR images (these rely upon the times for realignment of the local nuclear quadrupole moment following longitudinal and transverse magnetic field pulses).

The question of what 9D or 6D metric makes sense, in forming a measure of difference between DT tensors, has been considered in detail, particularly since any operation on such tensors must not only keep the symmetric nature of the arrays, but also their positive semi-definiteness property [5, 4, 7]. A particularly promising metric is the Log-Euclidean framework, which guarantees valid tensor results under filtering and other operations [5, 7]. In this simple scheme, tensor computations are carried out in the domain of matrix logarithms: we form the matrix logarithm (denoted Log) of a diffusion tensor \mathbf{D} via an SVD decomposition $\mathbf{D} = \mathbf{U} \mathbf{\Lambda} \mathbf{U}^T$ followed by the logarithm of the diagonal of the matrix $\mathbf{\Lambda}$ of eigenvalues:

$$\text{Log}(\mathbf{D}) = \text{Log}(\mathbf{U} \mathbf{\Lambda} \mathbf{U}^T) \equiv \mathbf{U} \log(\text{diag}(\mathbf{\Lambda})) \mathbf{U}^T \quad (1)$$

Note that since \mathbf{D} is symmetric positive semi-definite, \mathbf{U} is orthogonal and $\mathbf{\Lambda}$ is real, nonnegative. Zero eigenvalues in (1) are handled by truncating the number of columns of \mathbf{U} , and voxels that are all-zero return a zero $\text{Log}(\mathbf{D})$ matrix.

Then in this case a Euclidean metric is a proper definition of tensor dissimilarity [5]:

$$d(\mathbf{D}_1, \mathbf{D}_2) = \|\text{Log}(\mathbf{D}_1) - \text{Log}(\mathbf{D}_2)\| \quad (2)$$

In a neat formulation [5], we also notice that since off-diagonal elements of $\text{Log}(\mathbf{D})$ must be counted twice in eq. (2), we can go over to a completely traditional vector-difference formulation by vectorizing the upper triangular portion of matrix $\text{Log}(\mathbf{D})$ into a 6-vector, wherein the 4th to 6th components are multiplied by $\sqrt{2}$:

$$\begin{aligned} \mathbf{E} &= \text{Log}(\mathbf{D}), \\ \mathbf{v} &= (E_{11}, E_{22}, E_{33}, \sqrt{2}E_{12}, \sqrt{2}E_{13}, \sqrt{2}E_{23})^T \\ &= \text{vec}(\text{Log}(\mathbf{D})) \end{aligned} \quad (3)$$

(with the opposite transform when converting back to a matrix, dividing three of the vector components by $\sqrt{2}$).

Thus, to analyze DT data, we first convert every voxel matrix to a 6-vector.

ICA

As opposed to a more familiar Principal Component Analysis (PCA), ICA proceeds by seeking a minimally redundant, but non-orthogonal, set of basis functions. To do so, a set of maximally statistically *independent* basis

vectors is found. Independence is not simply decorrelation — PCA accomplishes that: the covariance approximates zero in the new basis coordinate system. Instead, independence means both decorrelation as well as the determination of signals, latent in the data, whose combinations equal the observed signals, such that the joint probability function amongst variables is factorizable into the product of marginal probability functions. This leads to the very strong result that the expectation value for the product of any functions of the new variables equals the product of expectation values of those functions of the new variables (see [23] for a tutorial introduction to the use of ICA in colour image compression).

Analyzing the whole-brain 6-vector dataset at once, suppose the resulting set of ICA basis vectors is \mathbf{B} . This is a $6 \times n$ matrix made up of set of n basis vectors \mathbf{b}_i , $i = 1..n$, where $n \leq 6$ is the dimensionality of the subspace in 6-space inhabited by a set of variables explaining the observed dataset in terms of latent processes or “sources”. ICA is a form of blind source separation that establishes both the subspace dimensionality n as well as the set of vectors \mathbf{B} . Vectors \mathbf{b} are not orthogonal, although they can be normalized. Therefore to form a set of coefficients \mathbf{c} that will act as the new set of variables in the new basis coordinate system, we must filter the 6-vector original data \mathbf{v} with an $n \times 6$ set of filters \mathbf{F} given by the pseudo-inverse of basis matrix \mathbf{B} :

$$\begin{cases} \mathbf{F} = \mathbf{B}^+, & \text{where } \mathbf{F} \mathbf{B} = \mathbf{I} \\ \text{coefficients:} & \mathbf{c} = \mathbf{F} \mathbf{v}, \\ & \mathbf{v} = \text{vec}(\text{Log}(\mathbf{D})) \\ \text{reconstituted 6-vector:} & \mathbf{v} = \mathbf{B} \mathbf{c} \end{cases} \quad (4)$$

Usually, in real medical data one finds that $n = 6$.

3. Diffusion Tensor Data and Perceptual Colour

To be concrete, let us consider DT data for brain scans¹. Fig. 1 shows both T1-weighted and one component of DT data for one slice of MR data from a dataset of $256 \times 256 \times 55$ voxels, i.e., each of 55 slices consists of a 256×256 array of data (the original data is of size 246×246 mm field-of-view at 2.2 mm slice thickness). The T1 data is spatially registered with the DT data; T1 data is scalar, whereas DT data is 6-dimensional, and in Fig. 1 we show T1 and the first DT component ($D_{1,1}$) for slice #25. All data is 32-bit floating point.

Since we have settled on the Log-Euclidean metric eq. (1) as representing a correct dissimilarity metric between DT voxel data, it is natural to map into the CIELAB perceptually-based colour metric: the reason is that, considering for example the (normalized) luminance component L^* of the L^*, a^*, b^* triple, stimulus is mapped into response using a 1/3 power law; but in fact the shape of the 1/3 power curve is very similar to that of a logarithm [17]. I.e., both CIELAB and other perceptually-driven metrics are manifestations of the well-known Weber’s Law in psychology, whereby equal perception of difference is proportional to equal percent difference: $\Delta \text{Response} \propto \Delta \text{Stimulus} / \text{Stimulus}$.

We carry out ICA using the Fastica algorithm [24], and find $n = 6$ basis 6-vectors. Fig. 2 shows the relative strengths of the six ICA coefficients c_1, c_2, \dots, c_6 , for the same slice as in Fig. 1. Here we order the six coefficients in

¹Here we make use of data available at <http://lbam.med.jhmi.edu/>



Figure 1. Brain MR data: (a): T1-weighted (scalar); (b): Diffusion tensor (component $D_{1,1}$).

order of overall variance of the c_i (as one can do in deciding how to quantize multi-dimensional data [23]). The data has negatives, since it is combinations of $\text{Log}(\mathbf{D})$ data, so has been shifted to non-negative for display, by adding one overall constant to all coefficients. In order to carry out ICA, we first find voxels with non-zero values, and take the 2-dimensional spatial convex hull, to restrict the set of data to just the brain and not the background, as in Fig. 2(g), so as to not influence the ICA procedure by the background. Fig. 2(h) shows the coefficient value statistics: they are all non-negative for c_1 , but all have median zero for the other components, and are smaller.

Having decided to map the $\text{Log}(\mathbf{D})$ metric into the CIELAB metric, how indeed should we map 6D log-diffusion tensor information into 3D CIELAB vectors? Here, we argue that we can utilize the output of an ICA decomposition to help us decide how to map into colour.

In the first place, DT data is diagonally dominant, and nonnegative. Hence we can reasonably expect that the most important ICA component c_1 will be nonnegative. Indeed, that does turn out to be the case for the (whole-brain) data being examined in Fig. 1. If we code “brightness” via this first ICA component, then the rest of the 6D information can be coded using “colour”. In this way, we code the main information into the visual channel with the most acuity, and reserve colour as a modulating factor encoding the remaining ICA information. Thus we suggest coding $c_1 \rightarrow L^*$, $\{c_2..c_6\} \rightarrow \{a^*, b^*\}$.

The question then revolves around how to map the 5D information not contained in c_1 into 2D colour. Examining the variances associated with the other basis subspaces, they present no distinguished features, for the data we examined, so we cannot simply take another two ICA components as our colour content.

The information not contained in c_1 consists of the reconstituted vectors \mathbf{v} , as in eq. (4), minus the part belonging to the \mathbf{b}_1 subspace, $c_1 \mathbf{b}_1$. Again, this new, 5-dimensional subspace has no clear distinguished directions (the SVD shows the 5D subspace to be fairly spherical). Therefore we take another tack, and carry out a second ICA analysis on the information orthogonal to \mathbf{b}_1 . In this way, the main feature in the remaining data information is captured in the lead component found, in a type of projection pursuit scheme. If we then go on to perform a third and final ICA calculation on the 4D subspace resulting from subtraction of this result, we will arrive at three orthogonal 6-vectors that best characterize the 6D information in three vectors. The resulting schema is therefore as follows:

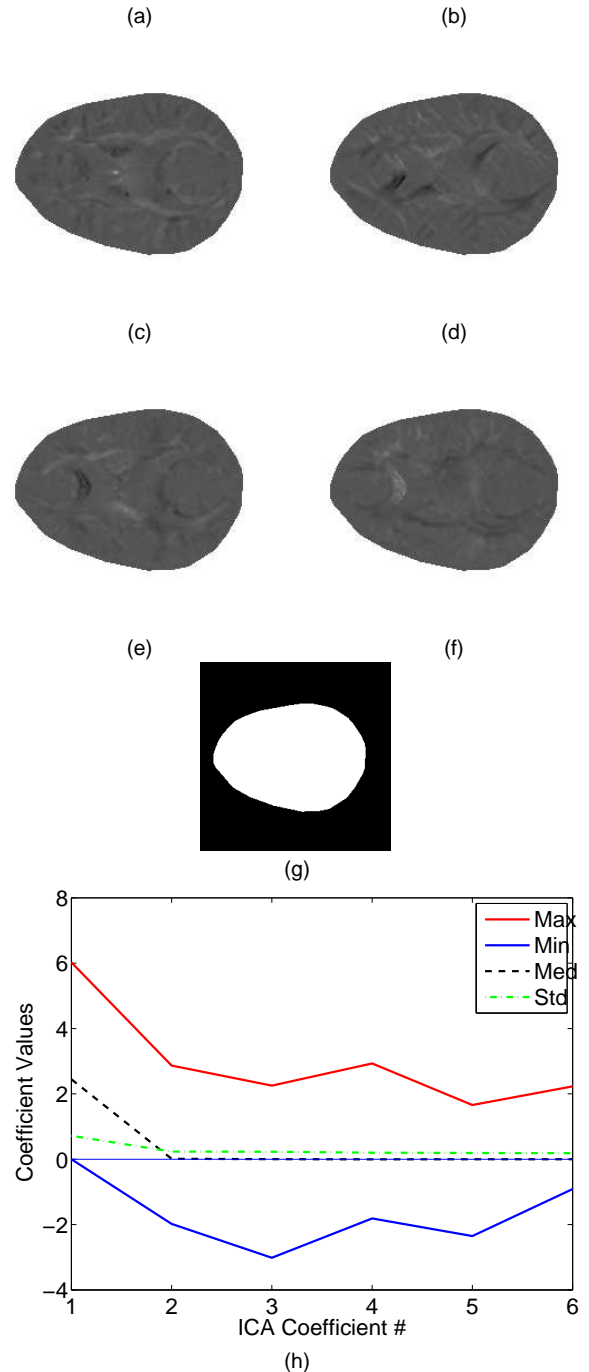


Figure 2. Whole-brain 6-dimensional ICA components for $\text{Log}(\mathbf{D})$, for one slice. (a) to (f): c_i , $i = 1..6$; (g): ICA is carried out on the pixels within the convex hull of non-zero $\text{Log}(\mathbf{D})$ values. (h): Minimum (blue), maximum (red), median (black, dashed), and standard deviation (green, dot-dashed) of c_i , $i = 1..6$.

Carry out ICA on $\mathbf{v} = \text{Log}(\mathbf{D})$ data.

Form coefficients $\mathbf{c} = \mathbf{F} \mathbf{v}$, where $\mathbf{F} = \mathbf{B}^+$ is the set of ICA filters corresponding to basis set \mathbf{B} .

Sort basis set in descending order by variance of coefficients c_i .

Coefficient $c_1 = \mathbf{f}_1^T \mathbf{v}$, where \mathbf{f}_1 is the first row of $\mathbf{F} = \mathbf{B}^+$.

Form data set orthogonal to \mathbf{b}_1 :

$$\mathbf{v}' = \mathbf{v} - c_1 \mathbf{b}_1.$$

Repeat ICA analysis, but on 5D subspace formed by \mathbf{v}' .

$$\text{Coefficient } c'_1 = (\mathbf{f}'_1)^T \mathbf{v}'.$$

Remove contribution of c'_1 and repeat ICA:

$$\mathbf{v}'' = \mathbf{v}' - c'_1 \mathbf{b}'_1; c''_1 = (\mathbf{f}''_1)^T \mathbf{v}''$$

Identify the primary ICA basis vectors with perceptual colour:

$$L^* \leftarrow c_1; a^* \leftarrow c'_1; b^* \leftarrow c''_1.$$

Note that we now have three orthonormal analysis 6-vectors associated with colour, as follows:

$$\begin{aligned} \vec{L} &= \mathbf{f}_1 \\ \vec{a} &= \mathbf{f}'_1 \\ \vec{b} &= \mathbf{f}''_1 \end{aligned}$$

Adjust magnitudes of a^*, b^* such that

$\text{Log}(\mathbf{D})$ metric eq. (2) is exactly mapped into CIELAB:

$$L^* = (\mathbf{f}_1)^T \mathbf{v},$$

$$a^* = (\mathbf{f}'_1)^T \mathbf{v},$$

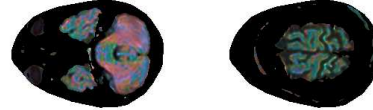
$$b^* = (\mathbf{f}''_1)^T \mathbf{v};$$

$$g = \sqrt{\|\mathbf{v}\|^2 - (L^*)^2},$$

$$h = g / \sqrt{(a^*)^2 + (b^*)^2},$$

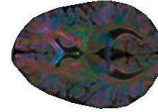
$$a^* = h a^*,$$

$$b^* = h b^*.$$



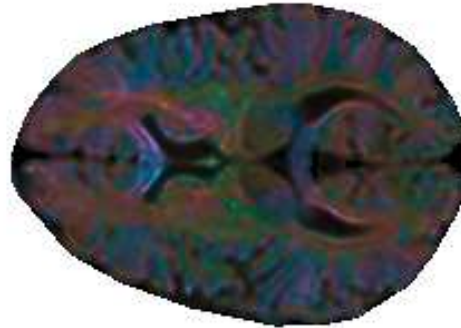
(a) slice 5

(b) slice 50



(c) slice 24

(d) slice 26



(e) slice 25

Figure 3. sRGB values for slices near slice 25 in Fig. 2 (as well as 5^t h. and 50^t h. slice): (a): slice 1; (b): slice 24; (c): slice 26; (d): slice 50; (e): slice 25.

For example, now the slice data depicted in Fig. 2 is coloured as in Fig. 3. To derive colour from CIELAB, we first convert to XYZ tristimulus coordinates. Then we go over to a linear-sRGB colour space [25], since the sRGB standard includes conversion from XYZ to sRGB. Finally, colours are shown in nonlinear sRGB to account for display gamma. A video of the sRGB for all 55 slices may be found at http://www.cs.sfu.ca/~mark/ftp/Cic15/DTsRGB_MP4V2.avi.

4. Application: Corpus Callosum Segmentation

Colour, as we have assigned it here to ICA processes, can be more expressive than the original data itself for tasks such as segmentation. The 6D tensor data does contain noise, which ICA ostensibly can remove. As well, ICA identifies the main information contained in the data.

As an example of the usefulness of colour, consider analyzing the variance within the standardized subdivision of the corpus callosum (CC), a nerve-fibres rich tissue connecting the brain hemispheres, into seven segments [26]. Fig. 4(a) shows a mid-sagittal (vertical) slice through the sRGB output of the method presented here: the CC stands out. The standard subdivision is shown in Fig. 4(b), where the contrast has been enhanced by correcting the tone curves — colours within the CC are histogram-equalized. Fig. 4(c) shows the whole slice with these tone curves. In contrast, consider the histogram-equalized FA measure, shown in Fig. 4(d). The FA has previously been used to distinguish the seven segments shown in Fig. 4(b) [27].

We can evaluate the utility of the colour mechanism proposed here as opposed to using the FA or the original

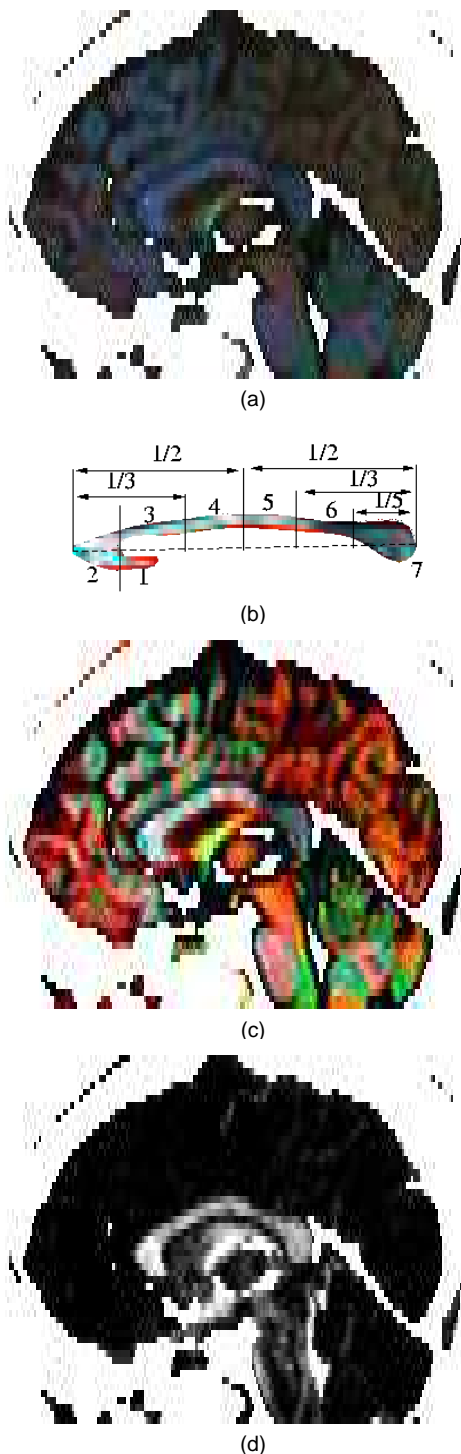


Figure 4. (a): Colour assigned to a vertical slice, displayed in sRGB: the CC stands out. (b): Standard segmentation of CC into seven sections. (c): Contrast-enhanced vertical segment. (d): FA (a scalar value), contrast enhanced.

data by carrying out an Analysis of Variance (ANOVA), with the null hypothesis that the means in all seven segments are the same. From Fig. 5(a) we see that the 95% confidence intervals for the means of the tensor data in the CC segments overlap substantially, making the original data not very dependable for segmentation purposes. The F-statistic for ANOVA is 22.6; the F-statistic is the ratio of between-group variance to within-group variance, with a larger F providing more evidence that the group means are distinguishable. In comparison, using the FA also generates overlapping means, as in Fig. 5(b); however the F-value improves to 29.9. But using colour, F is best, at 32.5: in Fig. 5(c) we see that at least one colour component does not overlap, between each segment, thus facilitating differentiating them. Nevertheless, for colour, for FA, and for the original data ANOVA reports that one can at least rule out the null hypothesis, with vanishingly small probability p-value.

To see how the seven segments look in CIELAB, Fig. 6 shows the $\{L^*, a^*, b^*\}$ coordinates for the seven CC segments (coloured using the mean sRGB colour from the CC in Fig. 4(b)). We can see a substantial change in CIELAB between segments.

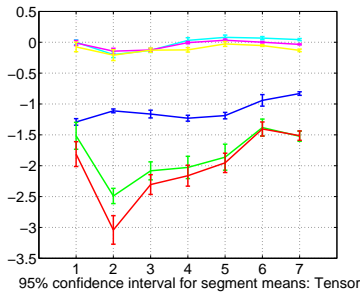
5. Conclusions

We have outlined a new colouring scheme for DT data, based on mapping a correct 6D tensor metric into perceptual colour coordinates in a reasonable way, guided by the ICA source separation mechanism.

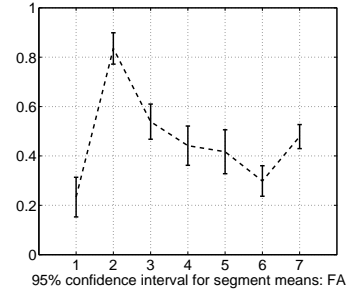
Future work will apply the method proposed here, capturing ICA information in a colour vector, to the task of tractography. Since this task amounts to a type of 3D segmentation, we will apply the Mean Shift approach to segmentation to the colour data developed here.

References

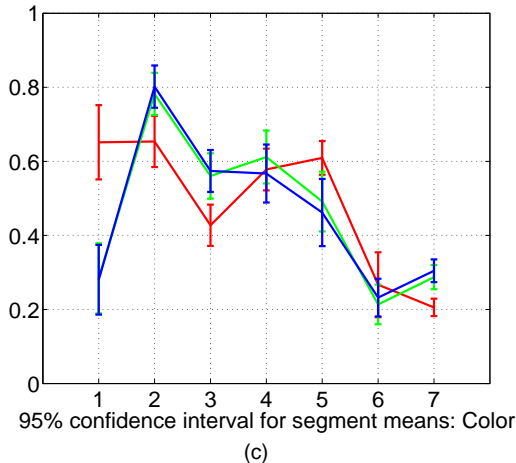
- [1] P.J. Basser, J. Mattiello, and D. LeBihan. MR diffusion tensor spectroscopy and imaging. *Biophys. J.*, 66:259–267, 1994.
- [2] D. Le Bihan. Looking into the functional architecture of the brain with diffusion MRI. *Nature Reviews Neurosci.*, 4:469–480, 2003.
- [3] E. Borning. Interactive deformations from tensor fields. In *IEEE Visualization '98*, 1998.
- [4] Z. Wang and B.C. Vemuri. DTI segmentation using an information theoretic tensor dissimilarity measure. *IEEE Trans. Med. Imaging*, 24:1267–1277, 2005.
- [5] V. Arsigny, P. Fillard, X. Pennec, and N. Ayache. Log-euclidean metrics for fast and simple calculus. *Mag. Res. in Medicine*, 56:411–421, 2006.
- [6] P.T. Fletcher and S. Joshi. Principal geodesic analysis on symmetric spaces: statistics of diffusion tensors. In *8th Euro. Conf. on Comp. Vision, Workshop on Comp. Vis. Approaches to Med. Image Anal. and Math. Methods in Biomed. Im. Anal.*, pages 87–98, 2004.
- [7] G. Hamarneh and J. Hradsky. Bilateral filtering of diffusion tensor MR images. In *IEEE Int. Symp. on Signal Proc. and Info. Tech.*, pages 507–512, 2006.
- [8] C. Pierpaoli, P. Jezzard, P.J. Basser, A. Barnett, and G. Di Chiro. Diffusion tensor MR imaging of the human brain. *Radiology*, 201:637–648, 1996.
- [9] M.R. Wiegell, H.B.W. Larsson, and V.J. Wedeen. Fiber crossing in human brain depicted with diffusion tensor MR imaging. *Radiology*, 217:897–903, 2000.
- [10] P.J. Basser and C. Pierpaoli. Microstructural and physiological features of tissues elucidated by quantitative-diffusion-tensor MRI. *J. Mag. Res.*, B111:209–219, 1996.



(a)



(b)



(c)

Figure 5. Means in the seven segments of the CC: (a): Original DT data; (b): FA data from Fig. 4(d); (c): Color data from Fig. 4(c).

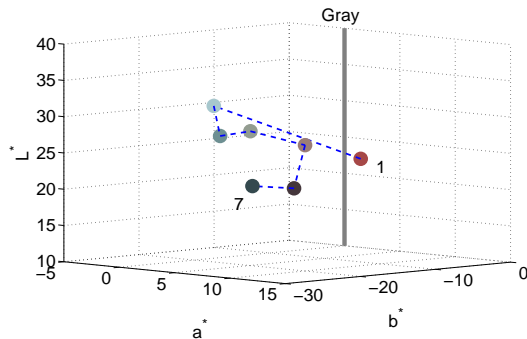


Figure 6. CIELAB coordinates for CC segments (coloured as in Fig. 4)

- [11] T. Beppu, T. Inoue, Y. Shibata, A. Kurose, H. Arai, K. Ogasawara, A. Ogawa, S. Nakamura, and H. Kabasawa. Measurement of fractional anisotropy using diffusion tensor MRI in supratentorial astrocytic tumors. *J. of Neuro-Oncology*, 63:109–116, 2003.
- [12] P.J. Basser, S. Pajevic, C. Pierpaoli, J. Duda, and A. Aldroubi. In vivo fiber tractography using DT-MRI data. *Mag. Res. in Medicine*, 44:625–632, 2000.
- [13] S. Pajevic and C. Pierpaoli. Colour schemes to represent the orientation of anisotropic tissues from diffusion tensor data: Application to white matter fiber tract mapping in the human brain. *Mag. Res. in Medicine*, 42:526–540, 1999.
- [14] G. Kindlmann, D. Weinstein, and D. Hart. Strategies for direct volume rendering of diffusion tensor fields. *IEEE Trans. on Vis. and Comp. Graphics*, 6:124–138, 2000.
- [15] T. Murata, S. Higano, H. Tamura, S. Mugikura, and S. Takahashi. Colour-coded fractional anisotropy images: Differential visualisation of white-matter tracts. *Neuroradiology*, 44:822–824, 2002.
- [16] G. Wyszecki and W.S. Stiles. *Color Science: Concepts and Methods, Quantitative Data and Formulas*. Wiley, New York, 2nd edition, 1982.
- [17] Z.-N. Li and M.S. Drew. *Fundamentals of Multimedia*. Prentice-Hall, 2004.
- [18] K. Arfanakis, D. Cordes, V.M. Haughton, J.D. Carew, and M.E. Meyerand. Independent component analysis applied to diffusion tensor MRI. *Mag. Res. in Medicine*, 47:354–363, 2002.
- [19] A. Hyvärinen, J. Karhunen, and E. Oja. *Independent Component Analysis*. John Wiley and Sons, Inc., New York, 2001.
- [20] J.-L. Hsu, J.-R. Duann, H.-C. Wang, and T.-P. Jung. Assessing rCBF changes in parkinson's disease using independent component analysis. In *4th Int. Symp. on Indep. Compon. Anal. and Blind Signal Sep. (ICA2003)*, pages 873–878, 2003.
- [21] M.A. Quigley, V.M. Haughton, J. Carew, D. Cordes, C.H. Moritz, and M.E. Meyerand. Comparison of independent component analysis and conventional hypothesis-driven analysis for clinical functional MR image processing. *Am. J. Neuroradiology*, 23:49–58, 2002.
- [22] S. Kim, J.-W. Jeong, and M. Singh. Estimation of multiple fiber orientations from diffusion tensor MRI. *IEEE Trans. on Nuc. Sci.*, 52:266–273, 2005.
- [23] M.S. Drew and S. Bergner. Spatio-chromatic decorrelation for color image compression. Technical report, Simon Fraser University, 2007. <http://fas.sfu.ca/pub/cs/TR/2007/CMPT2007-09.pdf>.
- [24] A. Hyvärinen and E. Oja. A fast fixed-point algorithm for independent component analysis. *Neural Computation*, 9(7):1483–1492, 1997.
- [25] International Electrotechnical Commission. Multimedia systems and equipment – colour measurement and management – part 2-1: Colour management – default RGB colour space – sRGB. IEC 61966-2-1:1999.
- [26] S.F. Witelson. Hand and sex differences in the isthmus and genu of the human corpus callosum: A post-mortem morphological study. *Brain*, 112:799–835, 1989.
- [27] K.M. Hasan, R.K. Gupta, R.M. Santos, J.S. Wolinsky, and P.A. Narayana. Diffusion tensor fractional anisotropy of the normal-appearing seven segments of the corpus callosum in healthy adults and relapsing-remitting multiple sclerosis patients. *J. Mag. Res. Imaging*, 21:735–743, 2005.